



# Spatial Scaling of End-stopped Perceptive Fields: Differences in Neural Bases of End-zones, Flanks and Centers

CONG YU,\*§ EDWARD A. ESSOCK\*+

Received 26 June 1995; in revised form 15 January 1996

**Length and width spatial interactions associated with a small test line centered on a rectangular background were measured at 0, 5 and 10 deg retinal eccentricities. Results indicated an elongated central region of summation with antagonistic flanks and end-zones comparable to earlier results [Yu, C. & Essock, E. A. (1996). *Vision Research* 36, 2883-2896]. The extent of the end-zones, flanks and centers (length and width) exhibited significantly different spatial scaling, which was steepest for the end-zones ( $E_2 = 0.45$  deg), less steep for the flanks ( $E_2 = 0.77$  deg) and least steep for the centers ( $E_2 = 2.05$  deg). Perceptive fields measured with concentric circular stimuli showed center and surround scaling equivalent to center and flank scaling, respectively, in line target experiments. These results suggest that: (1) psychophysical end-stopping and flank-inhibition reflect different underlying cortical neural processes; and (2) the spatial interactions apparent on the conventional Westheimer paradigm are partly governed by cortical factors. Copyright © 1996 Elsevier Science Ltd.**

End-stopping Flank-inhibition Perceptive field Spatial scaling Westheimer paradigm

## INTRODUCTION

Simple, complex and hypercomplex cells were first distinguished by Hubel and Wiesel (1962,1965,1968) in cat and monkey striate cortex. Subsequent studies (e.g. Dreher, 1972; Schiller *et al.*, 1976; Gilbert, 1977; Murphy & Sillito, 1987) showed that end-stopping, the defining characteristic of hypercomplex cells, is present also in many simple and complex cells. Hypercomplex cells are now viewed as subsets of simple and complex cells and are referred to as end-stopped or end-inhibited cells (e.g. Bolz & Gilbert, 1986; Murphy & Sillito, 1987). A typical end-stopped simple cell receptive field includes both inhibitory flanks and end-zones and is thus not only phase-sensitive, but also length-tuned.

Psychophysical end-stopping and flank-inhibition associated with line targets were demonstrated in increment threshold tasks with a modified Westheimer paradigm (Essock & Krebs, 1992; Essock *et al.*, 1997; Yu & Essock, 1993,1996). For a small target line centered on a rectangular background, the detection threshold is first elevated, then lowered, as the background size is

increased in either width or length. This classic pattern of desensitization followed by sensitization is taken to reflect local spatial interactions corresponding to a central region of summation surrounded by a region of antagonistic influence (Westheimer, 1965, 1967). Thus, with a line target, the desensitization and sensitization branches of the function obtained under the variable-length condition suggest central length summation and end-stopping, respectively, and those obtained under the variable-width condition suggest central width summation and flank-inhibition, respectively. Taken together, these end-zone, flank and central summation regions form an elongated end-stopped perceptive field which resembles a typical end-stopped simple cell receptive field. We have proposed that cortical end-stopped receptive fields may be the neural basis of these psychophysical expressions (Yu & Essock, 1996). This assumption is supported by the oblique effect of stronger psychophysical flank-inhibition (Essock & Krebs, 1992; Essock *et al.*, 1997) and end-stopping (Yu & Essock, 1996) observed at horizontal or vertical target orientations. This orientation bias suggests the involvement of cortical mechanisms (Mansfield, 1974; Essock, 1980).

In this psychophysical paradigm, end-stopping and flank-inhibition are functionally comparable, differing only in the locations (end-zones or sides) where they occur. On the other hand, compared to flank antagonism, receptive field end-stopping has been shown to be

\*Department of Psychology, University of Louisville, Louisville, KY 40292, U.S.A. †Department of Ophthalmology and Visual Science, University of Louisville, Louisville, KY 40292, U.S.A. §To whom correspondence should be addressed at: College of Optometry, University of Houston, Houston, TX 77204, U.S.A.

generated by distinct neural circuits, such as intracortical inhibition from cells with spatially offset receptive fields (e.g. Hubel & Wiesel, 1965; Bolz & Gilbert, 1986). Bolz and Gilbert (1986) demonstrated the disassociation of end-zone and flank-inhibition by pharmacologically abolishing end-inhibition while preserving flank properties. Accordingly, if psychophysical end-stopping and flank-inhibition are truly the behavioral expressions of receptive field properties, they would have different underlying neural mechanisms and therefore might exhibit distinct features under appropriate psychophysical test circumstances. Thus, the psychophysical disassociation of end-stopping from flank-inhibition, as well as from central summation, would be an important criterion to evaluate the validity of our assumption.

Measuring the scale change of the extent of a spatial property across various retinal eccentricities can provide information about whether the processing is limited by retinal or cortical factors (Levi *et al.*, 1985; Wilson *et al.*, 1990; Drasdo, 1991). This spatial scaling is often characterized by the value  $E_2$  defined by  $F = 1 + E/E_2$ , where  $F$  is the scaling factor indicating how a spatial property or performance varies,  $E$  is the retinal eccentricity, and  $E_2$  is the eccentricity at which the measured value is equal to twice the foveal value. Levi *et al.* (1985) and Wilson *et al.* (1990) suggested that the spatial scaling across eccentricity of a variety of visual tasks falls into two categories. Spatial scaling functions for tasks such as hyperacuity and spatial interaction have an  $E_2$  value in the range 0.3–0.9 deg, which matches the  $E_2$  values of cortical magnification in human (Cowey & Rolls, 1974) and monkey (Dow *et al.*, 1981). It is assumed that spatial abilities having  $E_2$  values comparable to that for cortical magnification (*c.* 0.8 deg) are limited by cortical factors (e.g. Wilson *et al.*, 1990). On the other hand, spatial scaling functions for tasks such as resolution acuity and contrast sensitivity have an  $E_2$  value in the range 1.5–4 deg, which matches the  $E_2$  values of cone and retinal ganglion cell spacing (*c.* 2.5 deg) and are presumed to be limited by retinal factors (Perry & Cowey, 1985). These values also match the  $E_2$  values of cortical receptive field center size (Dow *et al.*, 1981; Van Essen *et al.*, 1984), but the similar scaling of cortical receptive field center size and cone and retinal ganglion cell spacing suggests that cortical receptive fields receive their retinal input from a fixed number of neighboring cones and ganglion cells at any retinal eccentricity (Wilson *et al.*, 1990) and thus their spatial scaling is ultimately determined by retinal factors. Relatively shallow spatial functions, with  $E_2$  values in the range 1.5–2 deg, are often regarded as indicating performance being limited by retinal factors, and steep scaling functions, with  $E_2$  values in the range 0.3–0.9 deg, as reflecting a cortical limitation. For example, Toet and Levi (1992) reported that the  $E_2$  values for resolution of a T-shaped target and for spatial interactions between two such targets were approximately 2 deg and 0.2–0.4 deg, respectively. The dramatic scaling difference was attributed to retinal factors limiting the resolution of

these targets and cortical factors limiting their spatial interaction. Thus, spatial scaling can provide a way to psychophysically determine differences in neural limitations (i.e. retinal or cortical) of various visual processes. Furthermore, although there is no solid psychophysical evidence indicating that different cortical mechanisms must necessarily lead to significant differences of spatial scaling among tasks they support, Drasdo (1991) suggested that cortical magnification in different cortical areas, and cortical sampling by modular structures unevenly distributed within these areas, theoretically could create such differences.

In the present study, we extended our earlier studies on end-stopped perceptive fields (Yu & Essock, 1996) to measure their spatial scaling across retinal eccentricity. We anticipated that it would be possible to determine whether the spatial interactions of the end-stopped perceptive fields were limited by retinal or cortical factors, and also to differentiate spatial scaling among end-stopping, flank-inhibition and central summation. We measured spatial interactions in both the length and width dimensions at 0, 5 and 10 deg retinal eccentricities and determined the spatial scaling factors and  $E_2$  values of the end-zone, flank and central summation regions of the perceptive field. Our main purpose was to determine whether the end-stopping and flank-inhibition demonstrated psychophysically appear to have different neural bases, and thus support the assumption that they are the psychophysical correlates of cortical receptive field end-stopping and flank-inhibition. A second goal was to compare the mechanism underlying central summation and those underlying psychophysical end-stopping and flank-inhibition. As a control, we also measured the spatial scaling of the center/surround organization of circular perceptive fields associated with spot targets (Westheimer, 1965, 1967). By using both line and spot targets, we were able to compare the nature of the spatial interactions obtained with line targets (Yu & Essock, 1996) to those obtained in the original spot-target version. Brief reports of results in this paper were presented earlier (Yu *et al.*, 1995).

## GENERAL METHODS

### *Observers*

The same two subjects (one male and one female, both 30 yr old) served in all experiments. Both subjects were slightly myopic and wore appropriate lenses to correct their vision to 20/20 or better. Subject YC (one of the authors) was experienced in psychophysical observation. Subject HY had no prior psychophysical experience and was naive as to the purpose of the study. She was given considerable practice before the experiments formally started.

### *Apparatus and stimuli*

The stimuli were generated by a Vision Works computer graphics system (Vision Research Graphics, Inc.) and presented on a Nanao Flexscan 9080i color

monitor. The resolution of the monitor was 1024 x 512 pixels. Pixel size was 0.28 mm horizontal x 0.41 mm vertical. The frame rate was 117 Hz. Luminance of the monitor was made linear by means of an eight-bit look-up table (LUT). Viewing distance was varied for testing at the three retinal eccentricities to fit both fixation cross and stimuli on the screen, yet maximize the resolution of stimuli. Subjects were positioned by means of a chin rest at 5.64 m from the screen for foveal viewing, half of the foveal viewing distance (2.82 m) for 5 deg retinal eccentricity viewing and a quarter of the foveal distance (1.41 m) for 10 deg retinal eccentricity viewing. Viewing was monocular by the dominant eye (right eyes for both subjects) with a white translucent diffuser positioned before the other eye.

An increment test field and a background field were presented on the center of the monitor screen for foveal viewing or at the 5 deg and 10 deg retinal eccentricities on the temporal side of the horizontal meridian in the visual field for peripheral viewing. The test field was a target line centered on a rectangular background. In a given experiment, only one dimension (e.g. length or width) of the background field was varied and the other dimension was fixed. The sides of the rectangular background were parallel to the sides of the target line in all experiments. The test line and background were oriented vertically, except as noted below. The luminance of the monitor screen was constant ( $6.85 \text{ cd/m}^2$ ) throughout all experiments, as was the luminance of the rectangular background ( $30 \text{ cd/m}^2$ ). The luminance of the target line was varied by a staircase procedure as the dependent measure. Additional details are given in corresponding sections.

### Procedure

A successive two-alternative forced-choice (2AFC) procedure was used. The background was presented in each of the two intervals (1.1 sec each). In one of the two intervals, the target line was also presented, starting 420 msec after the onset of the background, lasting for 420 msec, and disappearing 260 msec before the background offset. There was no interruption between two intervals. In foveal viewing each trial was preceded by a fixation cross which disappeared 100 msec before the beginning of the trial. For peripheral viewing, the fixation cross was present throughout testing. Intervals were marked by tones with different frequencies. Another tone gave feedback on incorrect responses.

Each staircase consisted of four "practice" reversals and six experimental reversals. Each correct response lowered test field luminance by one step and each incorrect response raised test luminance by three steps. Step size was  $3.6 \text{ cd/m}^2$  at the first pair of practice reversals and  $1.8 \text{ cd/m}^2$  at the second pair. It was  $0.6 \text{ cd/m}^2$  throughout the experimental phase. The mean of six experimental reversals was used to estimate the increment threshold which was defined as the difference of target luminance at threshold and background luminance on a log scale [ $\log(\Delta L + L) - \log L$ ].

Besides the practice at the beginning of the study, each observer also had two to three sessions of practice before each peripheral experiment. One experimental session usually consisted of 9-13 background conditions presented in a random order and lasted for 50 to 60 min. Each data point was the mean of the thresholds from five to six replication sessions, and the error bars represent  $\pm 1 \text{ SEM}$ .

### EXPERIMENT 1: MEASUREMENT OF LOCAL SCALING FACTORS

Since visual spatial sensitivity declines with increasing retinal eccentricity due to reduced neural sampling (e.g. Rovamo & Virsu, 1979), it was desirable to equate the visibility of peripheral and foveal targets before we compared the perceptive fields at different retinal eccentricities. It has been shown also that spatial processing can be homogeneous across the visual field if the stimuli are appropriately scaled (Rovamo *et al.*, 1978; Koenderink *et al.*, 1978). Although estimating the scaling factor from cone or ganglion cell spacing was first thought to also reflect cortical magnification (Rovamo *et al.*, 1978), later studies suggested that retinal and cortical scales are quite different (Levi *et al.*, 1985; Wilson *et al.*, 1990; see Introduction). Therefore, it is inappropriate to scale the peripheral stimuli either with the cone or ganglion cell spacing data, or with cortical magnification factors, before we know whether processing is limited by retinal factors or by cortical factors. Alternatively, Johnston (1987) and Watson (1987) suggested that any particular aspect of visual processing can be equated at any two visual field locations by magnifying the stimulus with a (local) scaling factor. This local scaling factor (Watson, 1987) can be estimated by measuring the sensitivity to a stimulus which has an identical form and is varied only in its size. The estimation is independent of any prior estimates of cortical or retinal magnification, as well as any presumption of the neural basis of the visual processing.

In this experiment, we applied the concept of local scale and measured local scaling factors for line and spot targets. These scaling factors were used later in the following experiments to magnify peripheral stimuli to equate their visibility. In this experiment, the detection thresholds for a foveal 1x5' line and a 1' diameter spot (without the background field present) were measured, as was a series of their magnified forms at the 5 and 10 deg retinal eccentricities. The width and length of the foveal line and the diameter of the foveal spot were magnified by factors of 1.33, 2.00, 2.66, 3.33 and 4.00, respectively, at the 5 deg retinal eccentricity, and 2.00, 2.66, 3.33, 4.00 and 4.66, respectively, at the 10 deg retinal eccentricity. The luminance of the screen was  $30 \text{ cd/m}^2$ , the same as the background luminance in later experiments.

The peripheral data were fitted with an exponential equation,  $T = aM^b$ , where  $T$  refers to threshold,  $M$  to magnification factor, and  $a$  and  $b$  are free parameters. The magnification factors that produced thresholds which matched the foveal thresholds were taken as the local

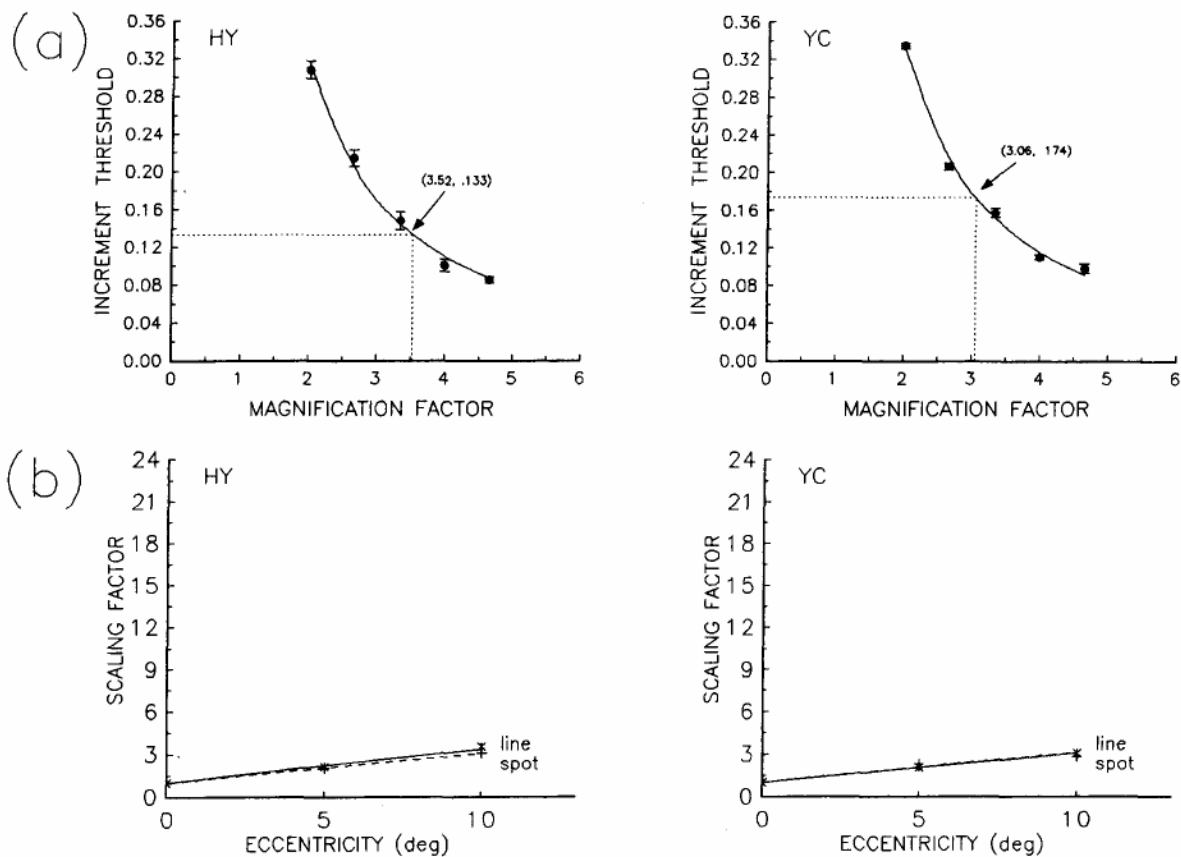


FIGURE 1. Local scaling factors used to magnify the sizes of peripheral stimuli for equal retinal sampling across retinal eccentricity, (a) An example of data fitting and local scaling factor derivation. Data were measured at the 10 deg retinal eccentricity for the line target. The raw data (filled circles) are first fitted by an exponential equation (see text). The fitted data (solid curve) are then matched with foveal threshold (indicated by the dotted horizontal line). The  $x$  value of the intersection point of the dotted horizontal line (foveal threshold) and solid curve (fitted data) is taken as the local scaling factor (indicated by the dotted vertical line), (b) Local scaling factors [as obtained in (a)] plotted as a function of the retinal eccentricity. Least-squares regression lines are plotted for line-only (x) and spot-only (+) targets.

scaling factors. Examples of this procedure are shown in Fig. 1(a). The  $E_2$  values in this and later experiments were calculated from the equation  $F = 1 + E/E_2$  given earlier. As seen from this function,  $E_2$  is actually the inverse of the slope of the eccentricity function, and thus is independent of any specific eccentricity. Local scaling factors plotted as a function of retinal eccentricity are shown in Fig. 1(b). For subject HY, the local scaling factor for the line target is 2.11 ( $E_2 = 4.51$  deg) at the 5 deg retinal eccentricity and 3.52 ( $E_2 = 3.97$  deg) at the 10 deg retinal eccentricity, and for the spot target is 2.02 ( $E_2 = 4.90$  deg) at the 5 deg retinal eccentricity and 3.06 ( $E_2 = 4.85$  deg) at the 10 deg retinal eccentricity. For subject YC, the local scaling factor for the line target is 2.06 ( $E_2 = 4.72$  deg) at the 5 deg retinal eccentricity and 3.06 ( $E_2 = 4.85$  deg) at the 10 deg retinal eccentricity, and for the spot target is 2.32 ( $E_2 = 3.79$  deg) at the 5 deg retinal eccentricity and 2.82 ( $E_2 = 5.49$  deg) at the 10 deg retinal eccentricity. As Fig. 1(b) indicates, each subject's spatial scaling functions for line and spot targets are linear and essentially identical. The  $E_2$  values from the two subjects fall into a range 3.79-5.49 deg, with an

overall mean value of 4.64 deg (the overall slope of the psychometric functions is about 0.22). These  $E_2$  values are about equal to Watson's (1987) estimation of local spatial scale in a contrast sensitivity function measurement using a similar procedure ( $E_2 = 4.17$  deg, recalculated from Watson, 1987).

#### EXPERIMENT 2: LENGTH SUMMATION AND END-STOPPING ACROSS RETINAL ECCENTRICITY

Length summation and end-stopping were measured first at the 0 deg retinal eccentricity for a 1 x 5' line superimposed on a 3'-wide rectangular background of various lengths. This was a replication of an earlier experiment (Experiment 2 Yu & Essock, 1996) and served as the baseline for later 5 and 10 deg retinal eccentricity length experiments. Because data collected from seven subjects in the earlier measurement had been very consistent, only five-six critical background length conditions were selected. Increment threshold as a function of background length is shown in Fig. 2(a). The length of central summation region (i.e. background length at which the peak threshold occurs) is about 11'

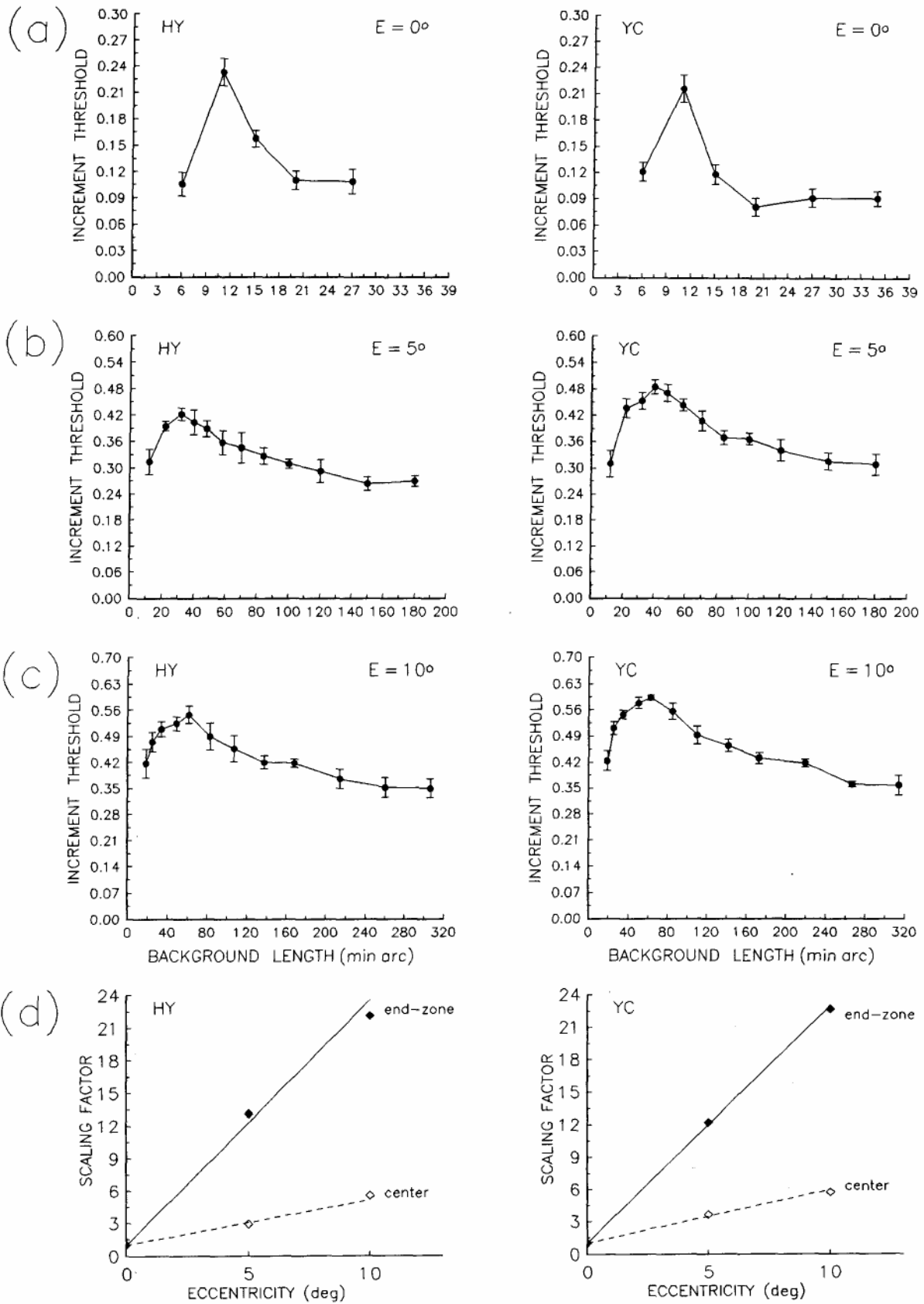


FIGURE 2. (a)-(c) Increment threshold plotted as a function of the length of the background field at 0, 5 and 10 deg retinal eccentricities. The rising portion of the function is taken to reflect length summation, and the declining portion reflects end-stopping. Note the scale of\* and y abscissas are different among figures (also in Figs 3 and 4). (d) Spatial scaling factors (ratio of peripheral data: foveal data) for the lengths of the center region and end-zone region of the perceptive field plotted as a function of the retinal eccentricity.

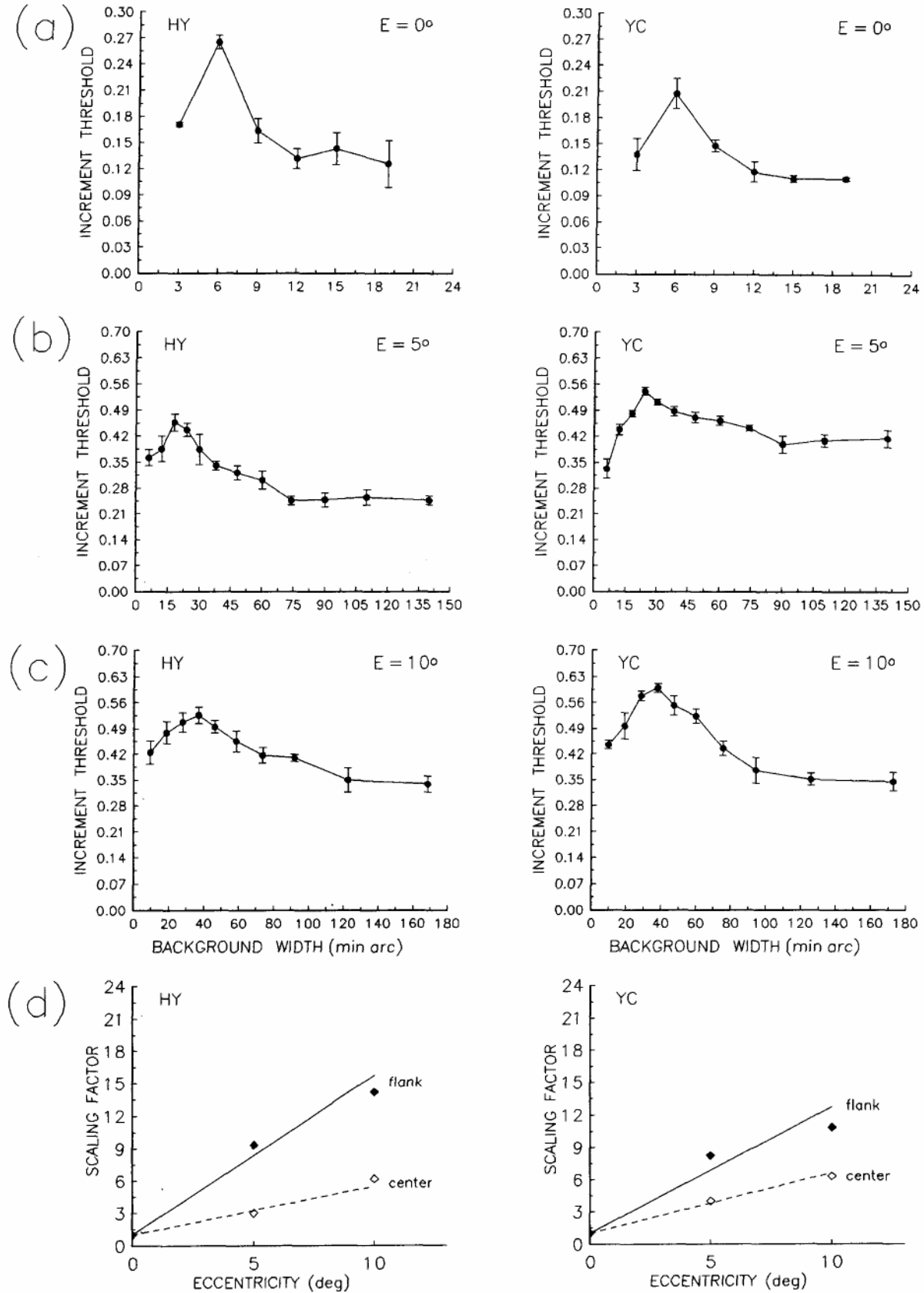


FIGURE 3. Spatial interaction functions and spatial scaling functions for a background of variable width plotted as in Fig. 2 for variable-length background. (a)-(c) Width summation and flank-inhibition at 0, 5 and 10 deg retinal eccentricities, (d) Spatial scaling factors for the width of the flank region and center region of the perceptive field plotted as a function of the retinal eccentricity.

long, and the length of the end-stopping region (half of the peak-to-plateau distance in terms of background length)\* is about 4.5' long, respectively, for the two subjects. These data are comparable to those reported in earlier measurements (Yu & Essock, 1996).

This test was then performed at the 5 and 10 deg retinal eccentricities. For each subject, the width and length of the target line and the width of the rectangular background were magnified by his/her corresponding local scaling factors of the line target determined in Experiment 1. Therefore, the stimulus configuration at the 5 deg eccentricity was a 2.11 x 10.55' line centered on a 6.33' wide background for HY and a 2.06 x 10.3' line centered on a 6.18' wide background for YC. At the 10 deg retinal eccentricity, it was a 3.52 x 17.60' line on a 10.56' wide background for HY and a 3.06 x 15.30' line on a 9.18' wide background for YC. Data collected at the 5 deg retinal eccentricity are plotted in Fig. 2(b). The length of the central summation region is 32' ( $F = 2.91$ ,  $E_2 = 2.62$  deg) for HY and 40' ( $F = 3.64$ ,  $E_2 = 1.90$  deg) for YC (where  $F$  is the ratio of peripheral data to foveal data and  $E_2$  is calculated from  $F$  based on the equation  $F = 1 + E_2$ ). The length of the end-stopping region is 59' ( $F = 13.11$ ,  $E_2 = 0.41$  deg) for HY and 55' ( $F = 12.22$ ,  $E_2 = 0.45$  deg) for YC. Data collected at the 10 deg retinal eccentricity are plotted in Fig. 2(c). The length of the central summation region is 61' ( $F = 5.55$ ,  $E_2 = 2.20$  deg) for HY and 63' ( $F = 5.73$ ,  $E_2 = 2.12$  deg) for YC. The length of the end-stopping region is 100' ( $F = 22.11$ ,  $E_2 = 0.47$  deg) for HY and 102' ( $F = 22.67$ ,  $E_2 = 0.46$  deg) for YC.

Figure 2(d) plots the scaling factor as a function of retinal eccentricity. Both subjects' data show the same trend. Spatial scaling factors for the end-zone and center both increase linearly with retinal eccentricity, but the increase in scaling for the end-zone size is much steeper than that for the center region. The average  $E_2$  value is about 0.45 deg for the end-zone (slope = 2.23) and 2.21 deg for the center (slope = 0.45). This scaling difference suggests that end-stopping and central summation may depend on different neural mechanisms.

### EXPERIMENT 3: WIDTH SUMMATION AND FLANK-INHIBITION ACROSS RETINAL ECCENTRICITY

The extent of width summation and flank-inhibition were first measured at the 0 deg retinal eccentricity for a 1 x 5' line superimposed on a 6'-long rectangular background with various widths. This was also a replication of an earlier experiment (Experiment 1, Yu & Essock, 1996) and set the baseline for later periphery experiments. Results are shown in Fig. 3(a). The widths of the central summation region (background width at which the peak threshold occurs) and the flank-inhibition region (half of the peak-to-plateau distance in terms of background

width) are about 6' and 3' for HY, and 6' and 4' for YC, respectively.

The same conditions were then tested at the 5 and 10 deg retinal eccentricities. The width and length of the target line and the length of the rectangular background were also magnified by each subjects' local scaling factors of line target. The line sizes were the same as in Experiment 2. The background length at the 5 deg retinal eccentricity was 12.66' for HY and 12.36' for YC. At the 10 deg retinal eccentricity it was 21.12' for HY and 18.36' for YC. However, both the target line and the background were set to horizontal in this measurement. The width of the background was thus varied vertically so that the retinal eccentricity would remain fairly constant, particularly when the background was very wide. Previous data (Yu & Essock, 1996) demonstrated that results from horizontal and vertical conditions do not differ.

Data collected at the 5 deg retinal eccentricity are plotted in Fig. 3(b). The width of the central summation region is 18' ( $F = 3.00$ ,  $E_2 = 2.50$  deg) for HY and 24' ( $F = 4.00$ ,  $E_2 = 1.67$  deg) for YC. The width of the flank-inhibition region is 28' ( $F = 9.33$ ,  $E_2 = 0.60$  deg) for HY and 33' ( $F = 8.25$ ,  $E_2 = 0.69$  deg) for YC. Data collected at the 10 deg retinal eccentricity are plotted in Fig. 3(c). The width of the central summation region is 37' ( $F = 6.17$ ,  $E_2 = 1.94$  deg) for HY and 38' ( $F = 6.33$ ,  $E_2 = 1.88$  deg) for YC. The width of the flank-inhibition region is 43' ( $F = 14.17$ ,  $E_2 = 0.76$  deg) for HY and 44' ( $F = 10.88$ ,  $E_2 = 1.01$  deg) for YC.

Figure 3(d) plots the scaling factor as a function of the retinal eccentricity. Similar to the length experiment data (Experiment 2), a linear spatial scaling can also be seen in the flank-width and center-width functions, although this relation for the flank function is less clear than that for the other data. The average  $E_2$  value is about 0.77 deg for flanks (slope = 1.31) and 2.00 deg for centers (slope = 0.50). That the flank function is much steeper than the center function suggests that flank antagonism and central summation may also depend on different neural mechanisms. The average  $E_2$  value for the summation center is 2.21 deg (Experiment 2) in the length dimension and 2.00 deg in the width dimension (current experiment), indicating that the summation center is homogeneous across both dimensions with respect to scaling.

### EXPERIMENT 4: CENTER/SURROUND SPATIAL INTERACTION FOR A SPOT TARGET ACROSS RETINAL ECCENTRICITY

Westheimer (1965, 1967) noted that the spatial interactions associated with a small spot target centered on a circular background appear to reflect center/surround organization comparable to that of a retinal ganglion cell receptive field. Numerous studies performed with both human and animal subjects using a variety of behavioral methods (e.g. Westheimer, 1965, 1967; Enoch & Sunga, 1969; Spillmann *et al.*, 1987) as well as single-unit recordings of retinal ganglion cells (Essock *et al.*, unpublished data) all support this assumption of a

\*The peak-to-plateau distance is halved to provide the length of each end-zone on the assumption of symmetrical end-zones.

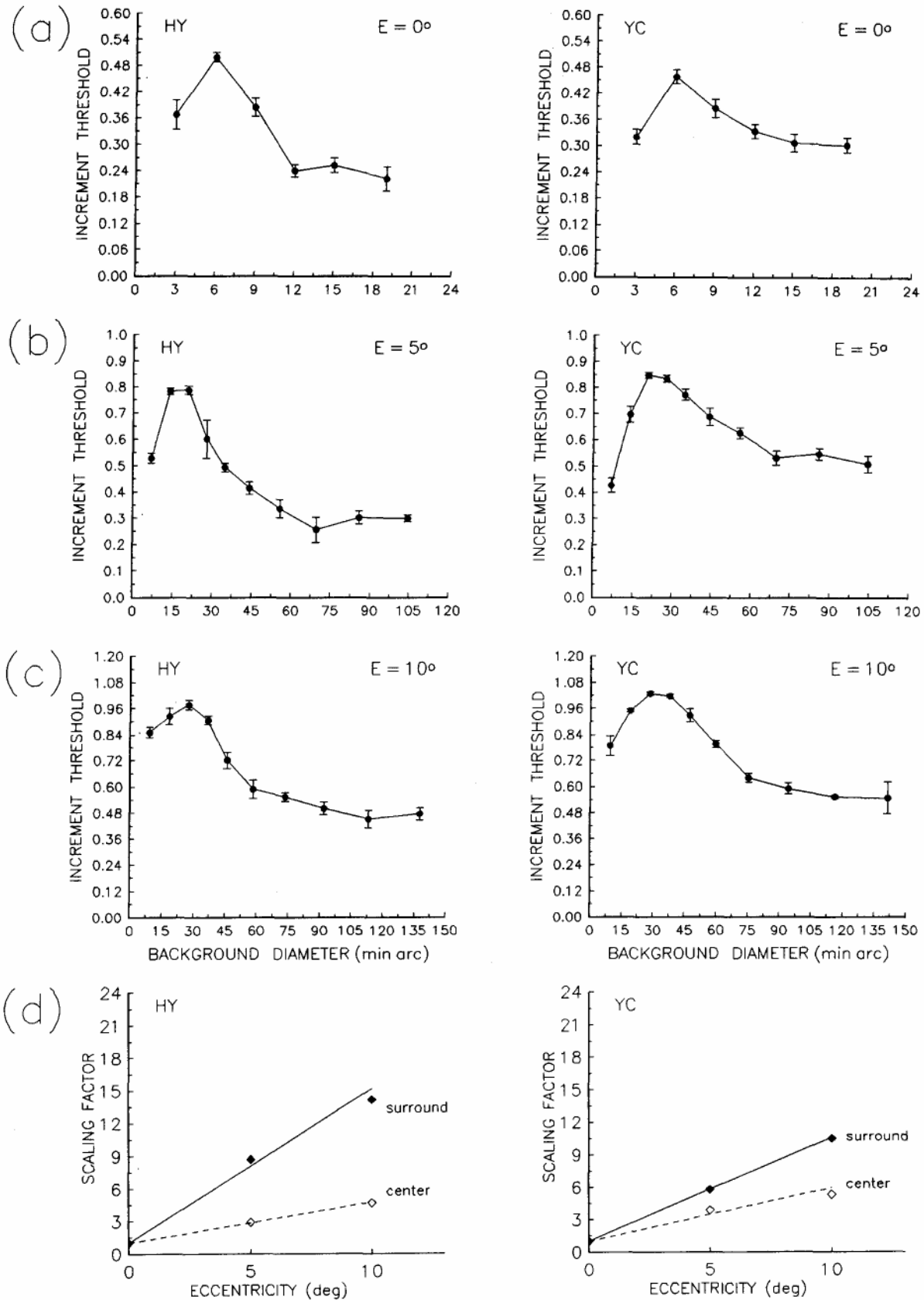


FIGURE 4. Spatial interaction functions and spatial scaling functions obtained for a circular spot target centered on a circular background of variable diameter. (a)-(c) Center/surround spatial interactions at 0,5 and 10 deg retinal eccentricities, (d) Spatial scaling factors for the sizes of center and surround region of the perceptive field plotted as a function of the retinal eccentricity.



relation of psychophysical spatial interactions and retinal ganglion cell receptive field properties. Several experiments measured the spatial interactions at different retinal eccentricities (Westheimer, 1967; Enoch, 1978; Spillmann *et al.*, 1987). Westheimer (1967) measured the spatial scaling of only the center of the perceptive field and found it to be about the same as the spatial scaling of resolution acuity. However, in his measurement the spot target was not magnified to equate its effective size at each retinal eccentricity, which may have resulted in retinal under-sampling and made the data less accurate. Spillmann *et al.* (1987) reported the spatial scaling of perceptive fields in both human and monkey. They found that sizes of the center and surround both increase with retinal eccentricity, and that the slope of the surround function is steeper.

In this experiment, we first measured central summation and surround antagonism at the 0 deg retinal eccentricity for a 1'-diameter spot centered on a circular background. Results are shown in Fig. 4(a). The diameter of the summation center (background diameter at which peak threshold occurs) and inhibitory surround on each side (half of the peak-to-plateau distance in terms of background diameter) are about 6 and 3', respectively, for HY, and 6 and 4', respectively, for YC\*. The same functions were then measured at the 5 and 10 deg retinal eccentricities. For each subject, the diameter of the spot target was magnified by his/her local scaling factor of the spot target (Experiment 1). This factor was 2.02' for HY and 2.32' for YC at the 5 deg retinal eccentricity and 3.06' for HY and 2.82' for YC at the 10 deg retinal eccentricity. Data collected at the 5 deg retinal eccentricity are plotted in Fig. 4(b). The size of the central summation region is 17' in diameter ( $F = 2.90$ ,  $E_2 = 2.63$  deg) for HY and 23' ( $F = 3.87$ ,  $E_2 = 1.74$  deg) for YC. The size of the surround-inhibition region is 26' ( $F = 8.70$ ,  $E_2 = 0.65$  deg) for HY and 23' ( $F = 5.80$ ,  $E_2 = 1.04$  deg) for YC. Data collected at the 10 deg retinal eccentricity are plotted in Fig. 4(c). The size of the central summation region is 28' in diameter ( $F = 4.67$ ,  $E_2 = 2.73$  deg) for HY and 32' ( $F = 5.33$ ,  $E_2 = 2.31$  deg) for YC. The size of the surround-inhibition region is 43' ( $F = 14.17$ ,  $E_2 = 0.76$  deg) for HY and 42' ( $F = 10.50$ ,  $E_2 = 1.05$  deg) for YC.

Figure 4(d) plots the scaling factors as a function of retinal eccentricity. It shows that the spatial scaling factors for the surround and the center both increase linearly with retinal eccentricity, and that the surround function is steeper than the center function. The average  $E_2$  value is 2.35 deg for center functions (slope = 0.43) and 0.88 deg for surround functions (slope = 1.14). The general trend of spatial scaling is comparable to Spillmann and colleagues' human and monkey data, which also showed steeper scaling in the surround function.

\*To be consistent with the values reported for rectilinear stimuli in Experiments 2 and 3, these values are reported as the full width (diameter) of the center and the extent of the surround on one side (i.e. the "thickness" of an annulus).

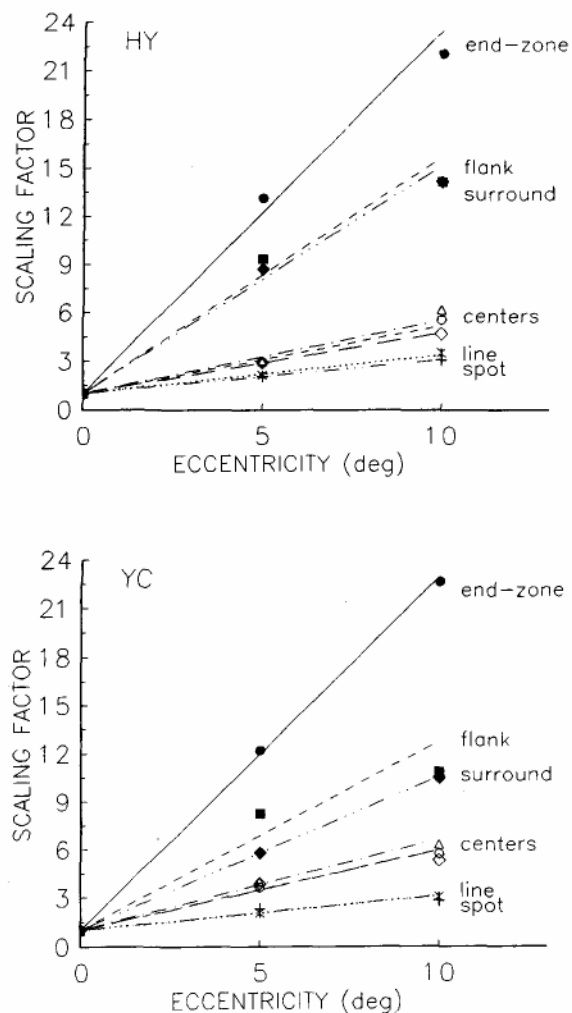


FIGURE 5. Summary of spatial scaling functions in each experiment replotted from earlier figures [Figs 1(b), 2(d), 3(d) and 4(d)]. The scaling functions fall into four groups: (1) end-zone scaling (filled circles); (2) antagonistic flank regions for a line target (filled squares) and antagonistic surround for a spot target (filled diamonds); (3) width (triangles) and length (circles) of center region for a line target and diameter (diamonds) of center region for a spot target; and (4) local scaling factors for line (x) and spot (+) targets.

## GENERAL DISCUSSION

In this study, the spatial scaling of spatial interactions was measured for elongated and circular perceptive fields across retinal eccentricity. Scaling for components of elongated perceptive fields (center width, center length, flank width and end-zone length) and components of circularly symmetric perceptive fields (center and surround sizes) were measured. When the spatial scaling functions in each experiment [Fig. 1(b), 2(d), 3(d) and 4(d)] are plotted together (Fig. 5), four categories of spatial scaling can be seen. The spatial scaling of end-zones is the steepest and stands out from the others. Next steepest is the spatial scaling of flanks (line target) and surrounds (spot target), which are very similar to each other and form a second category. The spatial scaling for center regions is the next steepest and forms a third

category, with equivalent scaling for length and width of elongated centers, and for diameter of circular centers. Center scaling is close to, but consistently steeper than, local scaling functions for increment threshold of line or spot stimuli (i.e. targets with no background present). These line and spot local scaling functions are identical to each other, the least steep, and form the fourth category.

Both the psychophysical end-stopping and flank-inhibition are most likely limited by cortical factors. The  $E_2$  values of 0.45 deg for end-stopping and 0.77 deg for flank-inhibition fall squarely into the 0.3-0.9 deg range (Levi *et al.*, 1985; Wilson *et al.*, 1990), corresponding to human cortical magnification, and cannot be explained by the much slower increase of cone and ganglion cell spacing across eccentricity. That these inhibitory processes reflect cortical organization is also supported by the earlier demonstrations of orientation anisotropies in end-stopping (Yu & Essock, 1996) and flank-inhibition (Essock & Krebs, 1992; Essock *et al.*, 1997). In addition, the large scaling difference between psychophysical end-stopping ( $E_2 = 0.45$  deg, slope = 2.23) and flank-inhibition ( $E_2 = 0.77$  deg, slope = 1.31) indicates that these two types of antagonism may themselves be based on different cortical mechanisms, a conclusion consistent with the neurophysiological differences between receptive field end-zones and flanks (see Introduction section), and further supported by more recent evidence that psychophysical end-stopping is more severely impaired than flank-inhibition in amblyopic eyes (Yu & Levi, 1996). Thus, we conclude that psychophysical end-stopping and flank-inhibition reflect two different types of cortical inhibitory processes which appear to be receptive field end-stopping and flank-inhibition. The scaling difference between psychophysical end-stopping and flank-inhibition demonstrates that measurement of psychophysical spatial scaling may be able not only to differentiate retinal and cortical visual processing, but also to distinguish visual functions constrained by different cortical mechanisms. Why psychophysical end-stopping has a steeper spatial scaling than flank-inhibition is not yet known. It might be due to the fact that the population of end-stopped cells is relatively small and thus a larger sampling or higher magnification factor (lower  $E_2$ ) would be required to equate the foveal and peripheral performances on tasks related to end-stopping.

The scaling of central summation shows functions that are much less steep in comparison to psychophysical end-stopping and flank-inhibition. This difference clearly indicates that the factors limiting central summation are different from those limiting end-stopping and flank-inhibition. However, whether central summation is limited by retinal or cortical factors cannot be decided by the spatial scaling function alone, since the width and length  $E_2$  values (2.21 and 2.00 deg) fall into the range (1.5-4 deg) corresponding to the spatial scaling of either cones, ganglion cells, or cortical receptive field center sizes (Levi *et al.*, 1985; Wilson *et al.*, 1990). This issue might be clarified by further dichoptic testing.

These findings indicate that even center/surround spatial interactions observed with circular stimuli are partly based on post-retinal processing. First, the center and surround spatial scaling functions obtained with a spot target are essentially identical to center (either width or length) and flank functions, respectively, measured with line targets, suggesting a correspondence between the center mechanisms and between the flank and surround mechanisms whether measured with spot or rectilinear stimuli. Since the  $E_2$  value of surround antagonism, like that of flank-inhibition, matches the  $E_2$  value of cortical magnification, a role of cortical processing is indicated. Second, both Spillmann and colleagues' and our data indicate that the size of the surround increases with retinal eccentricity at a higher rate than does the size of the center, whereas recent single-unit recordings of P and M macaque ganglion cells (Croner & Kaplan, 1995) indicate that center and surround sizes of neurons increase at the same rate. Thus, a post-retinal factor appears to affect the scaling factor of the surrounds observed on the conventional Westheimer paradigm. Based on these findings, we conclude that the weighting functions of the center/surround mechanisms inferred with the Westheimer paradigm include modification by some cortical, probably inhibitory process. That is, the exact shape of the Westheimer paradigm functions reflects some cortical influence in addition to retinal center/surround organization.

An alternative account of differences in spatial scaling has been presented by Whitaker *et al.* (1992a, b) who measured spatial scaling in a number of position and movement acuity tasks, including vernier acuity, bisection acuity, spatial interval discrimination, and referenced and unreferenced displacement detection. The enormous differences of  $E_2$  values across these tasks (over 100-fold) led them to propose that  $E_2$  values may be primarily decided by a task-dependent scale selection mechanism in the visual system, rather than by the locus of the visual system (e.g. retinal or cortical) or the particular neurological pathways (e.g. a particular cell type or subset of cells). In the current study, the role of task-dependence was obviated since functions (center, flank and end-zone) were measured in the same increment threshold task with an identical target. The dramatic scaling differences that we report for these different spatial interactions provide strong evidence that differences in scaling between different neural levels or pathways is an important factor in determining the psychophysical spatial scaling performance and  $E_2$  values.

## REFERENCES

- Bolz, J. & Gilbert, C. D. (1986). Generation of end-inhibition in the visual cortex via inter laminar connections. *Nature*, 320, 362-365.
- Cowey, A. & Rolls, E. T. (1974). Human cortical magnification factor and its relation to visual acuity. *Experimental Brain Research*, 21, 447-454.
- Croner, L. J. & Kaplan, E. (1995). Receptive fields of P and M ganglion cells across the primate retina. *Vision Research*, 35, 7-24.
- Dow, B. M., Snyder, A. Z., Vautin, R. G. & Bauer, R. (1981).

- Magnification factor and receptive field size in foveal striate cortex of the monkey. *Experimental Brain Research*, *44*, 213-228.
- Drasdo, N. (1991). Neural substrates and threshold gradients of peripheral vision. In *Vision and visual dysfunction* (Vol. 5, *Limits of vision*). London: Macmillan.
- Dreher, B. (1972). Hypercomplex cells in the cat's striate cortex. *Investigative Ophthalmology*, *11*, 355-356.
- Enoch, J. (1978). Quantitative layer-by-layer perimetry. *Investigative Ophthalmology and Visual Science*, *17*, 208-257.
- Enoch, J. & Sunga, R. (1969). Development of quantitative perimetric tests. *Documenta Ophthalmology*, *26*, 215-229.
- Essock, E. A. (1980). The oblique effect of stimulus identification considered with respect to two classes of oblique effects. *Perception*, *9*, 37<sup>^</sup>t6.
- Essock, E. A. & Krebs, W. K. (1992). Sensitization of a line target depends on orientation and temporal modulation. *Investigative Ophthalmology and Visual Science (Suppl.)*, *33*, 1349.
- Essock, E. A., McCarley, J. S., Sinai, M. J., Khang, B. G., Lehmkuhle, S., Krebs, W. K. & Yu, C. (1997). Extensions of the sustained-like and transient-like effects. In Lakshminarayanan V. (Ed.), *Basic and clinical applications of vision science*, Dordrecht, Netherlands: Kluwer Academic Press.
- Gilbert, C. D. (1977). Laminar differences in receptive field properties of cells in cat primary visual cortex. *Journal of Physiology*, *268*, 391-421.
- Hubel, D. H. & Wiesel, T. N. (1962). Receptive fields, binocular interaction and functional architecture in the cat's striate cortex. *Journal of Physiology*, *160*, 106-154.
- Hubel, D. H. & Wiesel, T. N. (1965). Receptive fields and functional architecture in two nonstriate visual areas (18 and 19) of the cat. *Journal of Neurophysiology*, *28*, 229-289.
- Hubel, D. H. & Wiesel, T. N. (1968). Receptive fields and functional architecture of monkey striate cortex. *Journal of Physiology*, *195*, 215-243.
- Johnston, A. (1987). Spatial scaling of central and peripheral contrast-sensitivity functions. *Journal of the Optical Society of America A*, *4*, 1583-1593.
- Koenderink, J. J., Bourman, M. A., Bueno de Mesquita, A. E. & Slappendel, S. (1978). Perimetry of contrast detection thresholds of moving spatial sine wave patterns. III. The target extent as a sensitivity controlling parameter. *Journal of the Optical Society of America*, *61*, 1530-1537.
- Levi, D. M., Klein, S. A. & Aitsebaomo, A. P. (1985). Vernier acuity, crowding and cortical magnification. *Vision Research*, *25*, 963-977.
- Mansfield, R. J. (1974). Neural basis of orientation perception in primate vision. *Science*, *186*, 1133-1135.
- Murphy, P. C. & Sillito, A. M. (1987). Corticofugal feedback influences the generation of length tuning in the visual pathway. *Nature*, *329*, 727-729.
- Perry, V. H. & Cowey, A. (1985). The ganglion cell and cone distributions in the monkey retina: Implications for central magnification factors. *Vision Research*, *25*, 1795-1810.
- Rovamo, J. & Virsu, V. (1979). An estimation and application of the human cortical magnification factor. *Experimental Brain Research*, *37*, 495-510.
- Rovamo, J., Virsu, V. & Nasanen, R. (1978). Cortical magnification factor predicts the photopic contrast sensitivity of peripheral vision. *Nature*, *271*, 54-56.
- Schiller, P. H., Finlay, B. L. & Volman, S. F. (1976). Quantitative studies of single-cell properties in monkey striate cortex. I. Spatiotemporal organization of receptive fields. *Journal of Neurophysiology*, *39*, 1288-1319.
- Spillmann, L., Ransom-Hogg, A. & Oehler, R. (1987). A comparison of perceptive and receptive fields in man and monkey. *Human Neurobiology*, *6*, 51-62.
- Toet, A. & Levi, D. M. (1992). The two-dimensional shape of spatial interaction zones in the parafovea. *Vision Research*, *32*, 1349-1357.
- Van Essen, D. C., Newsome, W. T. & Maunsell, J. H. R. (1984). The visual field representation in striate cortex of the macaque monkey: Asymmetries, anisotropies, and individual variability. *Vision Research*, *24*, 429-448.
- Watson, A. B. (1987). Estimation of local spatial scale. *Journal of the Optical Society of America A*, *4*, 1579-1582.
- Westheimer, G. (1965). Spatial interaction in the human retina during scotopic vision. *Journal of Physiology*, *181*, 812-894.
- Westheimer, G. (1967). Spatial interaction in human cone vision. *Journal of Physiology*, *190*, 139-154.
- Whitaker, D., Makela, P., Rovamo, J. & Latham, K. (1992). The influence of eccentricity on position and movement acuities as revealed by spatial scaling. *Vision Research*, *32*, 1913-1930.
- Whitaker, D., Rovamo, J., MacVeigh, D. & Makela, P. (1992). Spatial scaling of vernier acuity tasks. *Vision Research*, *32*, 1481-1491.
- Wilson, H. R., Levi, D., Maffei, L., Rovamo, J. & DeValois, R. (1990). The perception of form. In Spillmann, L. & Werner, J. S. (Eds), *Visual perception: the neurophysiological foundations*. San Diego: Academic Press.
- Yu, C. & Essock, E. A. (1993). Psychophysical end-zone inhibition demonstrated with the Westheimer paradigm. *Investigative Ophthalmology and Visual Science (Suppl.)*, *34*, 418.
- Yu, C. & Essock, E. A. (1996). Psychophysical end-stopping associated with line target. *Vision Research*, *36*, 2883-2896.
- Yu, C., McCarley, J. S. & Essock, E. A. (1995). Psychophysical end-stopping, flank-inhibition, and central summation of perceptive fields are based on different neural substrates. *Investigative Ophthalmology and Visual Science (Suppl.)*, *36*, 2146.
- Yu, C. & Levi, D. M. (1996). Psychophysical end-stopping and flank-inhibition: a consequence of intracortical inhibition. *Investigative Ophthalmology and Visual Science (Suppl.)*, *37*, 1334.

*Acknowledgement*—This research was supported by Fight-For-Sight grant GA90095.